www.elsevier.com/locate/csr

Spatial distribution and intra-annual variability of water masses on the Eastern Gulf of Cadiz seabed

M.J. Bellanco, R.F. Sánchez-Leal

PII: S0278-4343(16)30465-4
DOI: http://dx.doi.org/10.1016/j.csr.2016.09.001
Reference: CSR3480

To appear in: *Continental Shelf Research*

Received date: 3 January 2016
Revised date: 26 July 2016
Accepted date: 2 September 2016

Cite this article as: M.J. Bellanco and R.F. Sánchez-Leal, Spatial distribution and intra-annual variability of water masses on the Eastern Gulf of Cadiz seabed *Continental Shelf Research,* http://dx.doi.org/10.1016/j.csr.2016.09.001

Spatial distribution and intra-annual variability of water masses on the Eastern Gulf of Cadiz seabed.

M.J. Bellanco, R.F. Sánchez-Leal
Spanish Institute of Oceanography. Cadiz Oceanography Center. Puerto Pesquero, Muelle de Levante, s/n. E11006. Cadiz, Spain
mjbellanco@cd.ieo.es
rleal@cd.ieo.es

Abstract

This paper presents the spatial distribution and intra-annual variability of seabed hydrography in the Eastern Gulf of Cadiz based on more than 10 years of near-bottom CTD observations. Well-defined water masses and a variety of mixing products are persistently sorted along three bathymetric areas occupying particular depth intervals: (i) inner shelf waters (< 60 m depth), with strong coastal and atmospheric influence; (ii) low-salinity Eastern North Atlantic Central Waters (ENACW) related to the Gulf of Cadiz Current (GCC) along the central and outer shelf (between 100 and 250 m depth); and (iii) a range of salinity and temperature flavors associated with the dense Mediterranean Outflow Water (MOW) occupying the deeper grounds. All three are characterized by significant March– November hydrographic differences suggesting an intra-annual variability pattern. After summer heating and stratification of the water column, warm (17.8 ºC) and saline (36.26) waters occupy the inner-shelf in November whereas cooler (14.6 ºC) and less saline (36.17) waters occur in March as the combined result of the erosion of the seasonal thermocline and intensified continental runoff. Offshore, colder, more saline and hence denser MOW invades the upper slope in March diluting the easternmost tip of a saltier ENACW wedge and nudging its outer rim up onto the shelf. This narrows and constricts the GCC band in winter, while its bottom trace appears to broaden and stretch eastwards in November. More effective MOW-ENACW mixing west of the Strait of Gibraltar driven both by an elevated MOW and a less stratified ENACW could explain the winter salinification of most of the grounds deeper than 250 m.

Keywords

Gulf of Cadiz, seabed water masses; Thermohaline properties; Spatial distribution, intra-annual variability

1. Introduction

The Gulf of Cadiz is located off the Southwestern Iberian Peninsula, where the Atlantic Ocean and the Mediterranean Sea are connected through the Strait of Gibraltar. There, the water exchange is governed by a two-layered inverse estuarine circulation with Mediterranean Water (MW) flowing into the Gulf of Cadiz under Atlantic Water flowing into the Mediterranean Sea (e.g. Price et al., 1993).

The traditional view of the surface circulation in the Gulf of Cadiz poses a clockwise flow on the slope as part of a larger-scale anticyclonic gyre and a counter-current on the inner shelf (Folkard et al., 1997, Criado-Aldeanueva et al., 2006, Teles-Machado et al., 2007). The clockwise flow conveys both Eastern North Atlantic Central Waters (ENACW) from the Portuguese Coastal Transition Zone and the Azores Current towards the Mediterranean Sea (Sánchez and Relvas, 2003). The inshore counter-current transports waters westward during most of the year (Relvas and Barton, 2002, Sánchez et al., 2006). A number of mechanisms have been proposed as responsible for this pattern. Seasonal displacements of the Azores High have been related to the local upwelling-favorable winds (Fiúza et al., 1982) and its convergence to the Azores Current (Sánchez and Relvas,2003). Besides local wind forcing (Teles-Machado et al., 2007), alongshore pressure gradients (Relvas and Barton, 2002) generated by the spatially heterogeneous wind field (Sánchez et al., 2006; Garel et al., 2016) and the buoyancy flux associated with continental runoff (García-Lafuente et al., 2006) seem to be the trigger for the onset of the inshore coastal counter-current.

From the geomorphological point of view, the Gulf is characterized by a wide continental shelf. The continental slope presents a complex seafloor with channels, ridges, canyons and even mud volcanoes down to the abyssal plains (García et al., 2009). Whereas the lower slope and abyssal plain are dominated by down-slope processes that are partly detached from the upper slope region, the middle slope and its complex contourite depositional system are dominated by along-slope processes driven by the Mediterranean Outflow (MO)(Hernández-Molina et al., 2006).

After plunging past the Spartel Sill (360 m deep), the MO turns into an undercurrent that flows under the ENACW along the main channel axis of the Strait of Gibraltar with a salinity of 38.3 and temperature of 13.3 ºC (Gasser et al., 2011). The salinity wedge, initially about 10 km wide and 150 m thick, flows at speeds in excess of 1.5 m s^{-1} as a dense overflow (Ambar and Howe, 1979). The MO water (MOW) experiences a gradual decrease in temperature, salinity and velocity due to mixing and entrainment with the ENACW during the first 140 km of its pathway (Baringer and Price, 1997, Nash et al. 2012). After, it is seen to follow the seafloor morphology as a multi-branched bottom-trapped gravity current (Madelain, 1970) before reaching a neutral equilibrium depth past Cape St. Vincent.

The hydrographic study of such bottom-trapped features poses an inherent risk associated with taking conventional CTD observations near the ground. This work presents the first study of the Gulf of Cadiz hydrography based on the analysis of temperature and salinity observations taken at less than 2 m above the ground from a CTD attached to a bottom trawl gear. This dataset permits to gain insight in a little-known domain with energetic bottom-attached flows influenced by a complex bathymetry.

The paper is organized as follows: section 2 introduces the data and methodology, section 3 shows the main results for the water masses present near-bottom (section 3.1), their spatial distribution (section 3.2) and intra-annual variability (section 3.3), section 4 discusses the main results and section 5 summarizes the conclusions.

2. Data and methods

Since 1992 the Cadiz Center of the Spanish Institute of Oceanography (IEO), has been carrying out a series of semiannual bottom trawl cruises in the Gulf of Cadiz. These are usually conducted in late winter (around February-March) and early autumn (between October and November) and are aimed at studying demersal and benthic communities living on the continental shelf and slope (from approximately 15 m to 800 m depth) between 6º 20'W and 7º 20'W (figure 1).

Starting from March 2005 a Seabird 37-SM CTD is routinely being attached to the bottom trawl headline to provide salinity, temperature and pressure data along the trawling track. This CTD has a pumped circuit to improve the conductivity response. Every 10 seconds the pump flushes out the conductivity cell and brings a new water sample. The CTD is mounted in the central-left part of the trawling headline. Therefore, the measurements are located at a maximum height of 2 m over the ground (as determined by the net mouth vertical opening). The design of the bottom trawl gear (Baka 44/60) forces the headline to move ahead of the footrope. As a consequence, CTD measurements are not greatly affected by re-suspension of sediment generated during the trawling. At the nominal trawling speed of 3 knots this instrument provides measurements at 5 m intervals with an accuracy better than 0.005 ºC, 0.02 in salinity and 1 dbar in pressure.

Only CTD observations taken after the trawl gear contacted with the bottom and with a maximum net vertical opening less than 2 m were retained. Individual measurements were geo-referenced using cable length and the ship's attitude and navigation data. After that step, data was visually screened and edited to leave out outliers, inconsistent or suspicious values and unreliable net performance. This resulted in a grand total of 216617 observations (table 1) distributed over the study area along a number of trawling tracks (figures 1 and 2).

Observations were gridded on a 0.0125º x 0.0125º grid with the Data-Interpolating Variational Analysis (DIVA). DIVA allows optimal data spatial interpolation on a finite element grid, taking into account coastline and bathymetry and providing an estimate of the interpolation error (full description of the method is provided in Troupin et al., 2010).

The determination of the correlation length (L) and the signal-to-noise ratio (SNR) is of special importance to DIVA gridding. L is translated as the distance over which given data influence its neighborhood. The SNR gives an indication of the confidence one can have in data. Thus, it measures the closeness between the data and the analysis (Troupin et al., 2010). Ideally, SNR and L should be objectively determined by a cross-validation (Troupin et al., 2012). Given the heterogeneous distribution of data (figures 1 and 2), with large amount of closely-spaced observations taken along trawling tracks, we decided to subjectively trial-and-error relax the rather conservative cross-validation L and SNR estimates to values that rendered physically realistic thermohaline fields (0.4º L and 0.2 SNR), while keeping low interpolation errors.

DIVA has been applied both for the overall dataset and the subsets (March and November). Data were then gridded with large data voids masked in accordance with the interpolation error. These gridded fields were used to illustrate the spatial distribution of thermohaline properties near the ground, their intra-annual variability and provide a hint about the bottom

circulation patterns in the Eastern part of the Gulf of Cadiz.

In this work, in addition to temperature and salinity, density and spiciness has been used to present the results. Spiciness is a state variable that refers to spatial variations in the temperature and salinity of sea water, being largest for hot and salty water (spicy). This state variable is ideally suited for the description of the boundary between different water masses, such as, shelf-slope and coastal upwelling fronts, or marginal seas outflows. The spiciness has been calculated following the algorithm developed by Flament (2002).

The bathymetry data used in this work come from the GEBCO 1' grid (http://www.gebco.net/data_and_products/gridded_bathymetry _data/gebco_one_minute_grid) merged with a local multi-beam bathymetry (MB INDEMARES; IEO. 2012).

3. Results

3.1. Near-bottom water masses in the Gulf of Cadiz.

Figure 3 shows the scatter plots of all θ-S pairs together with the 1900-2007 mean θ-S profile at the central Gulf of Cadiz. This climatological mean was plotted for visual reference and was obtained from a database of hydrographic profiles provided by SeaDataNet (www.seadatanet.org).

Figure 3 (A) shows that the study area is occupied by two well-defined water masses and a number of mixing products. A cloud of water types falls along the near-straight line that joins temperatures between 12.5-16.0 ºC, salinities between 35.8-36.5 and densities between 26.7-27.1 kg m^{-3}. This water mass is a local modification of the ENACW, as described by Ambar

et al.(2002). Although exposed to significant intra-annual variability, this water mass occupies grounds shallower than 250 m both in March and November (figure 3; B and C panels).

Water with densities > 27.1 kg m^{-3} correspond to a wide variety of MW types with temperature between 13-15 ºC and salinity in excess of 36.2. These types, commonly known as MOW, are a consequence of mixing between MW-ENACW and are sorted by density and hence depth. On grounds deeper than 550 m the more saline MOW types occur, with salinities greater than 36.8. On the contrary, warmer and less saline MOW occupy shallower grounds. Figure 3 (B and C panels) suggests that the confluence between MW and ENACW occurs where the bottom depth is around 250 m.

Waters over grounds shallower than 60 m are best discerned in the θ-S diagram in November (figure 3; A and C panels) when they feature temperature values > 17.0 ºC and salinities between 36.0-36.5, also exhibiting a broader distribution in the θ-S space.

The θ-S plots depict the distribution of water masses on a non-neutral surface (the ground) rather than providing information on the vertical stratification of the water column. A number of dissimilarities between water column properties at the central Gulf of Cadiz and near-bottom observations are evident (figure 3). A wider range of MOW types emerge in the latter. The less saline MOW types occur on the shelf-break, where mixing with upper-layer ENACW is possible. Deeper grounds are occupied by MOW types resembling those observed in the vicinity of the Strait of Gibraltar (e.g. Ambar and Howe, 1979). The latter suggests that in the study region the MOW is still behaving as a bottom-trapped gravity current that has not yet entrained enough ENACW volume to detach as a buoyant plume.

In November (figure 3C), θ-S observations are well-sorted in density and depth. On the

contrary, the presence of colder water on the shelf in March (figure 3B) makes that horizontal density gradients be smaller in late winter. These weaker gradients could provide more favorable conditions for lateral and diapycnal ENACW-MW mixing. As such, θ-S pairs distributed along the ENACW-MW mixing triangle exhibit a wider range of variability in March, with values distributed along a broader and more diffuse isopycnal boundary than in November. In fact, we selected the θ-S pairs located between 200 and 350 m depth spanning the 26.7-27.6 (March) and 26.9-27.4 (November) isopycnals.

3.2. Spatial distribution

The general pattern is that of temperature (salinity) gradually decreasing (increasing) with increasing depth, particularly offshore of the 100 m isobath. Three main depth-dependent zones are discerned (figure 4).

(i) Shelf grounds shallower than 60 m are characterized by the highest temperatures (generally > 15.5 ºC), salinities between 36-36.4 (figure 4 A and B), low densities (generally < 26.7 kg m^{-3}; figure 4C) and high spiciness (generally > 3.2 and up to 4; figure 4D). This coastal band is not spatially homogeneous with lower salinities and temperatures close to the main river mouths (Guadiana and Guadalquivir) than elsewhere in the upper shelf (see figure 1 for location details).

(ii) Most of the ENACW (figure 3) is located between 100-250 m, featuring a low salinity (S < 36.2), relatively cold (around 14.5 ºC) wedge stretching along the outer shelf (figure 4A and B). This band is clearly separated from the deeper and saltier grounds below by a sharp, well-defined haline front. At the upper margin of the ENACW domain, the haline gradients are smoother. This upper boundary is defined by a sharp temperature front centered at about 15.5 ºC. The ENACW wedge is best identified in the spiciness map (figure 4D) that allows the

observation of a relatively homogeneous band with spiciness < 3 extending between the mid-shelf and the shelf-break.

(iii) Grounds offshore from the 250 m isobath are largely dominated by a range of dense (> 27.1 kg m^{-3}) MOW types featuring temperatures < 14.5 ºC and salinities > 36.2 tightly attached to the bathymetric features (figure 4A and B). The spatial continuity of this saline band is disrupted at 36º 30'N, 7º 00'W by a prominent seafloor elevation (Guadalquivir ridge; Hernández-Molina et al., 2006) capped by a relatively low salinity patch (< 36.6; down to 0.2 fresher than the surroundings).

Past this ridge (see figure 1 for further location details) the MOW spreads horizontally, as illustrated by the cross-slope horizontal separation between the 36.2-36.8 isohalines (figure 4A). A branch with salinities > 36.6 stretches inshore of the ridge following the 300 m isobath and a meandering fork with salinities > 36.8 occupy the deeper grounds.

3.2.1. Spatial variability

Figure 4 (E, F, G and H panels) shows the associated standard deviation of the mean fields presented before, computed at 0.06º x 0.06º cells. Most of the variability occurs at the upper shelf (depth < 60 m) and along the shelf break between 200-450 m. The former is primarily associated with the large March-November temperature differences as will be shown in section 3.3. In fact, temperature deviations decrease with increasing depth, exceeding 1 ºC on the inner shelf, about 0.75 ºC along the shelf-break and below 0.25 ºC in the MOW domain (figure 4F). On the other hand, the variability between 200-450 m is mostly salinity-driven (figure 4D), showing deviations in excess of 0.12 along that depth interval.

3.3. Intra-annual variability

The spatial distribution of thermohaline properties in late winter and early autumn is shown in figure 5. In order to better illustrate March-November dissimilarities, the spatial fields of temperature and salinity differences are presented in figure 6. In addition, table 2 shows estimates of the area-averaged temperature and salinity means together with the lower and upper bounds of the 95% confidence intervals for the parameter estimates of the normal distribution fitted to the original data (see table 2 for details).

In both seasons the three-band pattern is recurrent. However, following the expected seasonal cycle, in the shallower zone area-averaged temperatures and salinities are higher in November (figures 5, 6 and table 2) than in March (p-value for two-sample t-test on area-averaged temperature and salinity differences < 0.01, with 14.65 ºC and 36.17 in March and 17.78 ºC and 36.26 in November; table 2). Greater differences occur off the river mouths (figures 5 and 6). Hence, lighter waters occupy this inshore band in November whereas in late winter, colder, less-saline waters take over the inner shelf, particularly near to the river mouths, which is consistent with the impact of increased continental runoff between January-March (Lobo et al., 2004b).

The intermediate band is characterized by a low-salinity (< 36.2), low-spiciness (< 3.0) ENACW wedge (figure 5D and 5H) lying between 100-250 m depth. Although present both in March and November, this feature is narrower (figure 5A and E), cooler (figure 6B) and saltier (figure 6A) in March (p-value for two-sample t-test on area-averaged temperature and salinity differences < 0.05, with 14.41 ºC and 36.17 in March and 14.78 ºC and 36.12 in November; table 2).

Deeper grounds associated with the MOW exhibit a weak and marginally significant cooling and salinification in March (p-value for two-sample t-test on area-averaged temperature and salinity differences < 0.1, with 13.90 ºC and 36.64 in March and 14.01 ºC and 36.60 in November; table 2) that results in a denser winter MOW. Density maps (figure 5C and 5G) show that the 27.6 kg m^{-3} isopycnal extends farther onshore in late winter than in early autumn. The March salinity increase is ubiquitous with values greater than 0.15 at number of spots (figure 6A). Exceptions occur at localized regions (36º 40' N, 7º 10' W and 36º 10' N, 6º 45' W) although the scarcity of data in these locations render this result somewhat dubious (figure 2).

4. Discussion

On the Eastern Gulf of Cadiz seabed a number of water types are distributed along three well-defined areas occupying particular depth intervals: (i) a shallower zone with strong coastal and atmospheric influence; (ii) an intermediate zone occupied by low-salinity ENACW; and (iii) the deeper grounds featuring the MOW domain.

4.1. Shallower zone: grounds shallower than 60 m

Sedimentary records (Lobo et al., 2004), sequences of summer (e.g. Fiúza, 1983; Relvas and Barton, 2002) and winter SST satellite images (Sánchez et al., 2006) suggest that the average inshore circulation in the North-Eastern Gulf of Cadiz is dominated by a westward flow, sometimes called Gulf of Cadiz Coastal Counter Current (GCCC, Teles-Machado et al., 2007). Although the role of wind forcing on its generation cannot be disregarded (Teles-Machado et al., 2007; Criado-Aldeanueva et al., 2009; Garel et al., 2016) it seems that buoyancy inputs contribute to set up an alongshore pressure gradient that would help the development of a coastal westward flow (Relvas and Barton, 2002; García-Lafuente et al.,

2006; Sánchez et al., 2006). These buoyancy inputs may emerge as tidal pumping of warm water in summer (García-Lafuente et al., 2006), or by sudden river discharges (Sánchez et al., 2006), which are more frequent in winter (Lobo et al., 2004b).

Our results indicate that the inner-shelf is characterized by relatively low salinity and high temperature waters (figure 4),

in part modulated by the intra-annual variability of buoyancy inputs. Colder and less saline conditions occur in March, specially close to the main river mouths (figures 5 and 6) whereas warmer, lighter waters are found in November. This variability may be related to two types of processes. On one hand, due to the proximity to the coast, this region is exposed to river runoff and other buoyancy inputs of continental origin. And, on the other hand, these shallow grounds are within the extent of the surface mixed layer, for which air-sea interaction is expected to play a key role.

In winter, wind stirring is more intense (Criado-Aldeanueva et al., 2009) and more effective, since stratification of the water column is at its seasonal minimum (Navarro et al., 2006). In this situation, cooler and relatively fresher waters are homogeneous above the pycnocline and, on shallow grounds, from the sea surface down to the bottom.

In early autumn, following the expected seasonal stratification cycle, the surface mixed layer, which still retains warmer waters from the previous summer, increases its thickness reaching shallow grounds (Navarro et al., 2006). This warming together with a salinity increase is observed at the inner-shelf in November (figure 6).

Results derived from figures 5 and 6 reveal that a buoyancy gain through heating affects all the shallower zone in November, while cooling produces a buoyancy loss in March. However, close to the river mouths this general pattern of buoyancy loss is partially disrupted by

buoyancy inputs as a result of winter intensified river runoff.

4.2. Intermediate zone: 100-250 m

In the gap left between the coastal zone and the MOW domain, a wedge of low salinity, low spiciness ENACW is able to stretch parallel to the bathymetry along the shelf-break between 100-250 m and occupy the region bounded by these two energetic domains (figure 4).

We suggest that this low-salinity structure is the bottom signal of the clockwise Gulf of Cadiz Current (GCC) described by the numerical modeling study of Peliz et al. (2007). The GCC is a persistent, baroclinic, equatorward jet of ENACW flowing along the shelf break that develops as a response to the water exchange at the Strait of Gibraltar, part of which is entrained into the MO. The GCC exhibits a meandering behavior that may be associated with instabilities from a strongly sheared current over a complex topography (Peliz et al., 2009). This meandering behavior can be seen in the horizontal distribution of spiciness and salinity fields (figures 4 and 5).

Along its upper border the GCC features a diffuse (pronounced) separation with the upper zone in March (November), because water types occupying both zones bear strong similarities (differences; figure 5 and table 2). Instead, the GCC domain is clearly discerned from the saltier zone offshore by a sharp haline front caused by the GCC and MOW flowing with very different thermohaline properties in opposite directions (García-Lafuente et al., 2006; Peliz et al., 2009).

Although intra-annual variability is less pronounced at this depth interval than in the shallower zone, the ENACW wedge is narrower, cooler and more saline in March (figure 5A and 5E). It is hypothesized that winter GCC cooling and salinification is a result of the

interplay with the MOW flows below. This suggests a possible weakening of the GCC flow in late winter and intensification in November, as noted by Peliz et al. (2009).

4.3. Deeper zone: MOW domain

Grounds lying below 250 m are occupied by relatively cold (below 14.5 ºC) and saline (> 36.2) MOW tightly attached to the topographic features (figure 4A). Topographic steering (widely described in the literature; e.g. Zenk, 1975) may help to subdivide the MOW into different branches. Lower salinity patches (<36.60, figure 4A) suggest horizontal splitting of the MOW occurring over the Guadalquivir ridge and associated elevations, indicating the disrupting effect of topography on the MOW spreading.

The seasonality of the MO properties has been analyzed using different approaches by others (e.g. Bormans et al., 1986, Sammartino et al., 2015). These studies point out that the maximum outflow peaks around March-April and dwindles around September-October. Our results show that the MOW domain experiences a slight cooling and salinification (figures 5 and 6) that suggests a density increase in March (using results from table 2, area averaged density is 27.48 kg m^{-3} in March and 27.42 kg m^{-3} in November). These observations are in agreement with previous reports. Ambar et al. (2002), using two CTD datasets collected in the Gulf of Cadiz and in the Eastern Iberian Basin in September and January, observed higher salinities in winter relative to summer MW salinities. Likewise, García Lafuente et al. (2007), using CTD and current-meter time-series at the Spartel Sill of the Strait of Gibraltar, detected a seasonal cycle with cooler and denser waters leaving the Mediterranean Sea around April, in coincidence with the maximum outflow, and warmer and lighter waters around December-January.

Our results suggest that cooler, saltier and denser MOW flowing in winter through the Gulf

of Cadiz, practically in coincidence with the seasonal maximum outflow (Sammartino et al., 2015). Furthermore, winter decrease of ENACW-MOW density differences (e.g. Bormans et al., 1986; figure 3) occurs about in phase with more vigorous MO (Sammartino et al., 2015). An elevated MOW and less stratified thermocline waters above may contribute to a more effective MOW-ENACW mixing west of the Strait of Gibraltar and enhance lateral and diapycnal salt injection or detrainment (e.g., Mauritzen et al., 2001) towards a weakened ENACW wedge. This could explain the winter salinification of most of the grounds deeper than 250 m and onshore nudging and constriction of a GCC that broadens and stretches eastwards in November (figure 7).

5. Summary and conclusions

This paper presents the spatial distribution and intra-annual variability of seabed hydrography in the Eastern Gulf of Cadiz based on more than 10 years of near-bottom CTD observations. Well-defined water masses and a variety of mixing products are persistently sorted along three bathymetric areas occupying particular depth intervals: (i) inner shelf waters (< 60 m depth), with strong coastal and atmospheric influence; (ii) low-salinity ENACW related to the Gulf of Cadiz Current (GCC) along the central and outer shelf (between 100 and 250 m depth); and (iii) a range of salinity and temperature flavors associated with the dense MOW occupying the deeper grounds tightly constrained by the topography.

All three depth intervals are characterized by significant March-November hydrographic differences suggesting an intra-annual variability pattern. After the summer net heat gain and stratification of the water column, warm (17.8 ºC) and saline (36.26) waters occupy the inner-shelf in November whereas cooler (14.6 ºC) and slightly less saline (36.17) waters occur in March due to the erosion of the seasonal thermocline. This results in a buoyancy gain through

heating in November and a buoyancy loss caused by cooling in March. Nevertheless, this winter buoyancy loss is partially disrupted in some areas close to the river mouths by buoyancy inputs as a consequence of intensified river discharges during winter. These early autumn and late winter buoyancy inputs may contribute to set up an along-shore pressure gradients that stimulate the onset of the inshore counter-current.

Offshore, colder, more saline and hence denser MOW invade the upper slope in March (27.48 kg m^{-3} versus 27.42 kg m^{-3} in November) diluting the eastward most tip of a saltier ENACW wedge and nudging its outer rim up onto the shelf. This narrows and constricts the GCC band in winter, while its bottom trace appears to broaden and stretch eastwards in November. More effective MOW-ENACW mixing west of the Strait driven by an elevated MOW and a less stratified ENACW could explain the winter salinification of most of the grounds deeper than 250 m.

Intra-annual patterns observed in March and November in all three depth intervals largely reflect the forcing that took place during the previous weeks or even months, for this reason, we can call them as winter and late summer-early autumn characteristic patterns.

The hydrographic study of bottom-trapped features poses an inherent risk associated with taking conventional CTD profiles near the seafloor (they usually extend down to a few meters above the ground). By taking advantage of the quality controlled, geolocated trawl gear mounted CTD observations, we have been able to analyze and gain direct insight in a domain that was previously just indirectly explored. This also provides a first characterization of essential habitats of both sessile and vagile benthic species, which is essential both to understand the environmental covariates featuring its spatial distribution and to provide the keys explaining the seasonal timing and main features of their life-history traits, strategies and

tactics.

Acknowledgments

The financial support for this study was provided by the Spanish Oceanographic Institute through a PhD grant. We thank Ignacio Sobrino and other ARSA cruise chief scientists and the crews of the R/V Cornide de Saavedra and R/V Miguel Oliver for their work through these years. We are indebted to Carlos Farias and the scientific and technical IEO staff that helped to collect and maintain the dataset used in this study. We would also like to thank Marcos Llope, Marina Delgado and Fernando Ramos for sharing their ideas about statistical analysis and their scientific-technical assistance. We are indebted to J.L. Pelegrí and two anonymous reviewers for their helpful comments and suggestions, which have greatly contributed to improve the quality of this manuscript. DIVA is freely available for download at http://modb.oce.ulg.ac.be/viewsvn. This is a contribution to INGRES3 project (CTM2010-21229), STOCA (IEO2009), PESCADIZ (IEO2008) FARCO (P12-RNM-1953) and DILEMA (CTM2014-59244-C3-2-R) projects.

References

Ambar, I., Howe, M., 1979. Observations of the mediterranean outflow-II. The deep circulation in the vicinity of the Gulf of Cadiz. Deep Sea Research Part A. Oceanographic Research Papers 26 (5), 555–568.

URL http://www.sciencedirect.com/science/article/pii/019801497 900967

Ambar, I., Serra, N., Brogueira, M., Cabeçadas, G., Abrantes, F., Freitas, P., Gonçalves, C., Gonzalez, N., 2002. Physical, chemical and sedimentological aspects of the Mediterranean outflow off Iberia. Deep Sea Research Part II: Topical Studies in Oceanography 49 (19), 4163–4177, canary Islands, Azores, Gibraltar Observations (Canigo) Volume {II}: Studies of

the Azores and Gibraltar regions. URL http://www.sciencedirect.com/science/article/pii/S096706 4502001480

Baringer, M. O., Price, J. F., 1997. Mixing and Spreading of the Mediterranean Outflow. Journal of Physical Oceanography 27 (8),1654 – 1677. URL http://dx.doi.org/10.1175/15200485(1997)027<1654:MASOTM>2.0.CO;2

Bormans, M., Garrett, C., Thompson, K., 1986. Seasonal variability of the surface inflow through the Strait of Gibraltar. Oceanologica Acta 9 (4), 403 – 414.

Criado-Aldeanueva, F., García-Lafuente, J., Navarro, G., Ruiz, J., 2009. Seasonal and interannual variability of the surface circulation in the eastern Gulf of Cadiz (SW Iberia). Journal of Geophysical Research: Oceans 114 (C1). URL http://dx.doi.org/10.1029/2008JC005069

Criado-Aldeanueva, F., García-Lafuente, J., Vargas, J. M., Río, J. D., Vázquez, A., Reul, A., Sánchez, A., 2006. Distribution and circulation of water masses in the Gulf of Cadiz from in situ observations. Deep Sea Research Part II: Topical Studies in Oceanography 53 (11–13), 1144 – 1160, the Gulf of Cadiz Oceanography: A Multidisciplinary View The Gulf of Cadiz Oceanography: A Multidisciplinary View. URL http://www.sciencedirect.com/science/article/pii/S0967064506001019.

Fiúza, A., 1983. Upwelling Patterns off Portugal. In: Suess, E., Thiede, J. (Eds.), Coastal Upwelling Its Sediment Record. Vol. 10B of NATO Conference Series. Springer US, pp. 85–98. URL http://dx.doi.org/10.1007/978-1-4615-6651-9$_5$.

Fiúza, A., Macedo, M., Guerreiro, M., 1982. Climatological space and time variation of the Portuguese coastal upwelling. Oceanologica Acta 5, No 1, 31–40.

Flament, P., 2002. A state variable for characterizing water masses and their diffusive stability: spiciness. Progress in Oceanography 54 (1–4), 493 – 501. URL http://www.sciencedirect.com/science/article/pii/S0079661102000654

Folkard, A. M., Davies, P. A., Fiúza, A. F. G., Ambar, I., 1997. Remotely sensed sea surface thermal patterns in the Gulf of Cadiz and the Strait of Gibraltar: Variability, correlations, and relationships with the surface wind field. Journal of Geophysical Research: Oceans 102 (C3), 5669–5683. URL http://dx.doi.org/10.1029/96JC02505

García, M., Hernández-Molina, F., Llave, E., Stow, D., León, R., Fernández-Puga, M., del Río, V. D., Somoza, L., 2009. Contourite erosive features caused by the Mediterranean Outflow Water in the Gulf of Cadiz: Quaternary tectonic and oceanographic implications. Marine Geology 257 (1–4), 24 – 40. URL http://www.sciencedirect.com/science/article/pii/S0025322708002806

García-Lafuente, J., Delgado, J., Criado-Aldeanueva, F., Bruno, M., del Río, J., Vargas, J. M., 2006. Water mass circulation on the continental shelf of the Gulf of Cádiz. Deep Sea Research Part II: Topical Studies in Oceanography 53(11–13), 1182-1197. URL http://www.sciencedirect.com/science/article/pii/S09670645 06001032

García-Lafuente, J., Sánchez Román, A., Díaz del Río, G., Sannino, G., Sánchez Garrido, J. C., 2007. Recent observations of seasonal variability of the Mediterranean outflow in the

Strait of Gibraltar. Journal of Geophysical Research: Oceans 112 (C10), n/a–n/a. URL http://dx.doi.org/10.1029/2006JC003992

Garel, E., Laiz, I., Drago, T., Relvas, P., 2016. Characterisation of coastal counter-currents on the inner shelf of the gulf of cadiz. Journal of Marine Systems 155, 19 – 34. URL http://www.sciencedirect.com/science/article/pii/S0924796315001864

Gasser, M., Pelegrí, J., Nash, J., Peters, H., García-Lafuente, J., 2011. Topographic control on the nascent Mediterranean outflow. Geo-Marine Letters 31 (5-6), 301–314. URL http://dx.doi.org/10.1007/s00367-011-0255-x

Hernández-Molina, F., Llave, E., Stow, D., García, M., Somoza, L., Vázquez, J., Lobo, F., Maestro, A., del Río, V. D., León, R., Medialdea, T., Gardner, J., 2006. The contourite depositional system of the Gulf of Cádiz: A sedimentary model related to the bottom current activity of the Mediterranean outflow water and its interaction with the continental margin. Deep Sea Research Part II: Topical Studies in Oceanography 53 (11–13), 1420 – 1463. URL http://www.sciencedirect.com/science/article/pii/S0967064506001159

IEO. 2012. Caracterización física y ecológica del área marina de “Chimeneas de Cádiz“. LIFE+ INDEMARES. IEO-FB.

Lobo, F., Sánchez, R., González, R., Dias, J., Hernández Molina, F., Fernández-Salas, L., del Río, V. D., Mendes, I., 2004. Contrasting styles of the Holocene highstand sedimentation and sediment dispersal systems in the northern shelf of the Gulf of Cadiz. Continental Shelf Research 24(4–5), 461–482. URL http://www.sciencedirect.com/science/article/pii/S0278434303002504

Lobo, J., Plaza, F., Gonzáles, R., Dias, J., Kapsimalis, V., Mendes, I., Rio, V.D., 2004b. Estimations of bedload sediment transport in the Guadiana estuary (SW Iberian Peninsula) during low river discharge periods. Journal of Coastal Research 41, 12–26. Special Issue.

Madelain, F., 1970. Influence de la topographie du fond sur l'ecoulement Mediterraneen entre le Detroit de Gibraltar et le Cap Saint-Vincent. Cahiers Oceanographiques 22(1), 43–61.

Mauritzen, C., Morel, Y., Paillet, J., 2001. On the influence of Mediterranean Water on the Central Waters of the North Atlantic Ocean. Deep Sea Research Part I: Oceanographic Research Papers 48 (2), 347 – 381. URL http://www.sciencedirect.com/science/article/pii/S0967063700000431.

Nash, J. D., Peters, H., Kelly, S. M., Pelegrí, J. L., Emelianov, M., Gasser, M., 2012. Turbulence and high-frequency variability in a deep gravity current outflow. Geophysical Research Letters. 39 (18), n/a–n/a, l18611. URL http://dx.doi.org/10.1029/2012GL052899

Navarro, G., Ruiz, J., Huertas, I.E., García, C.M., Criado-Aldeanueva, F., Echevarría, F., 2006. Basin scale structures governing the position of the deep fluorescence maximum in the Gulf of Cádiz. Deep Sea Research II 53 (11–13), 1261–1281. URL http://www.sciencedirect.com/science/article/pii/S096706450600107X

Peliz, A., Dubert, J., Marchesiello, P., Teles-Machado, A., 2007. Surface circulation in the Gulf of Cadiz: Model and mean flow structure. Journal of Geophysical Research: Oceans 112 (C11). URL http://dx.doi.org/10.1029/2007JC004159

Peliz, A., Marchesiello, P., Santos, A. M. P., Dubert, J., Teles- Machado, A., Marta-Almeida, M., Le Cann, B., 2009. Surface circulation in the Gulf of Cadiz: 2. Inflow-outflow coupling and the Gulf of Cadiz slope current. Journal of Geophysical Research: Oceans 114 (C3). URL http://dx.doi.org/10.1029/2008JC004771

Price, J. F., Baringer, M. O., Lueck, R. G., Johnson, G. C., Ambar, I., Parrilla, G., Cantos, A., Kennelly, M. A., Sanford, T. B., 1993. Mediterranean outflow mixing and dynamics. Science 259(5099),1277–1282. URL http://www.sciencemag.org/content/259/5099/1277

Relvas, P., Barton, E. D., 2002. Mesoscale patterns in the Cape São Vicente (Iberian Peninsula) upwelling region. Journal of Geophysical Research: Oceans 107 (C10), 28–1–28–23. URL http://dx.doi.org/10.1029/2000JC000456

Sammartino, S., García Lafuente, J., Naranjo, C., Sánchez Garrido, J. C., Sánchez Leal, R., Sánchez Román, A., 2015. Ten years of marine current measurements in espartel sill, strait of gibraltar. Journal of Geophysical Research: Oceans, n/a–n/a. URL http://onlinelibrary.wiley.com/doi/10.1002/2014JC010674/abs tract

Sánchez, R., Mason, E., Relvas, P., da Silva, A., Peliz, A., 2006. On the inner-shelf circulation in the northern Gulf of Cádiz, southern Portuguese shelf. Deep Sea Research Part II: Topical Studies in Oceanography 53 (11–13), 1198 – 1218. URL http://www.sciencedirect.com/science/article/pii/S0967064506001044

Sánchez, R. F., Relvas, P., 2003. Spring–summer climatological circulation in the upper layer in the region of Cape St. Vincent, Southwest Portugal. ICES Journal of Marine Science: Journal du Conseil 60 (6), 1232–1250. URL

http://icesjms.oxfordjournals.org/content/60/6/1232.

Teles-Machado, A., Peliz, A., Dubert, J., Sánchez, R. F., 2007. On the onset of the Gulf of Cadiz Coastal Countercurrent. Geophysical Research Letters 34 (12). URL http://dx.doi.org/10.1029/2007GL030091

Troupin, C., Machín, F., Ouberdous, M., Sirjacobs, D., Barth, A., Beckers, J.-M., 2010. High-resolution climatology of the northeast Atlantic using Data-Interpolating Variational Analysis (Diva). Journal of Geophysical Research: Oceans 115 (C8). URL http://dx.doi.org/10.1029/2009JC005512

Troupin, C., Barth, A., Sirjacobs, D., Ouberdous, M., Brankart, J.-M., Brasseur, P., Rixen, M., Alvera-Azcárate, A., Belounis, M., Capet, A., Lenartz, F., Toussaint, M.-E., Beckers, J.-M., 2012. Generation of analysis and consistent error fields using the Data Interpolating Variational Analysis (DIVA). Ocean Modelling 52–53(0),90–101. URL http://www.sciencedirect.com/science/article/pii/S1463500312000790

Zenk, W., 1975. On the Mediterranean outflow west of Gibraltar. Meteor Forsch Ergebnisse A 16, 23–34.

Figures

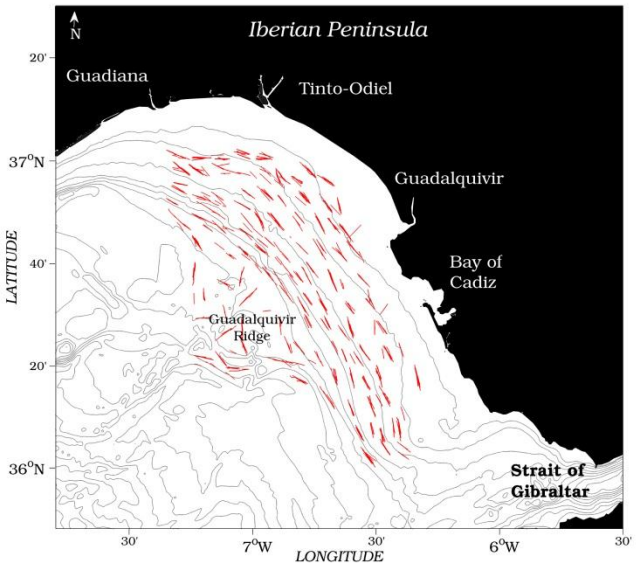

Figure 1: Location of the study area: Eastern Gulf of Cadiz (SW Iberian Peninsula). Red lines indicate the trawling tracks since March 2005. Bathymetry is depicted at 100 m intervals. The 25 m and 50 m isobaths are also shown.

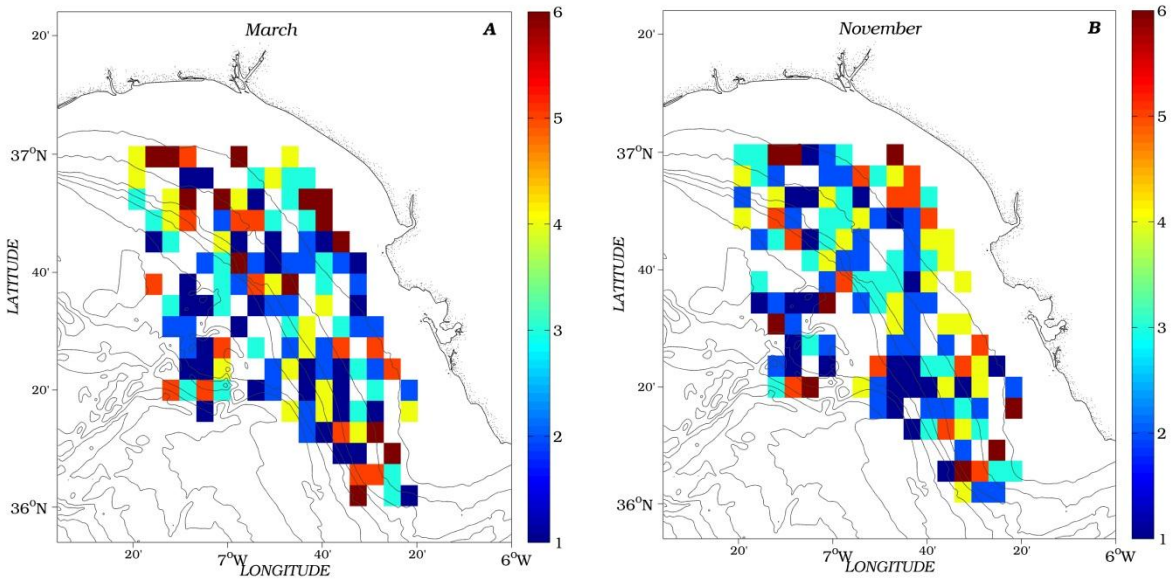

Figure 2: Distribution of hauls in 0.06º x 0.06º cells in March (A) and November (B). Colorbar indicates the number of hauls per cell. Bathymetry is depicted at 100 m intervals. The 50 m isobath is also shown.

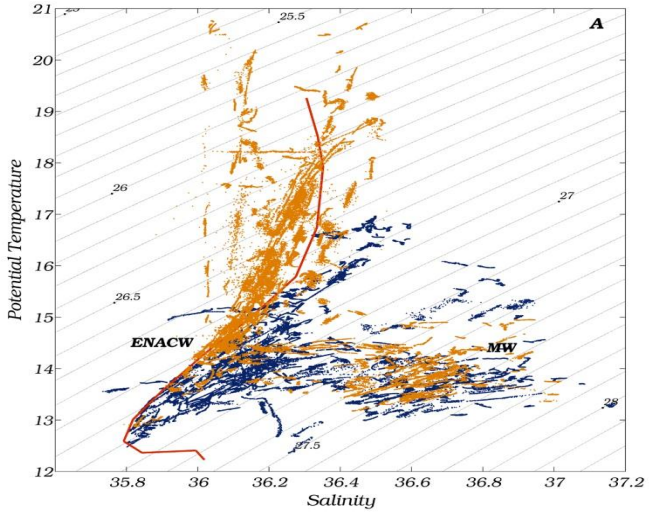

Figure 3: (A) Potential Temperature-Salinity (θ-S) diagram of the whole dataset (November data in orange, March data in blue). The red line indicates the climatological mean θ-S curve (1900-2007), at 7.6ºW, 36.5º N.

ENACW and MW are the acronyms for Eastern North Atlantic Central Water and Mediterranean Water.

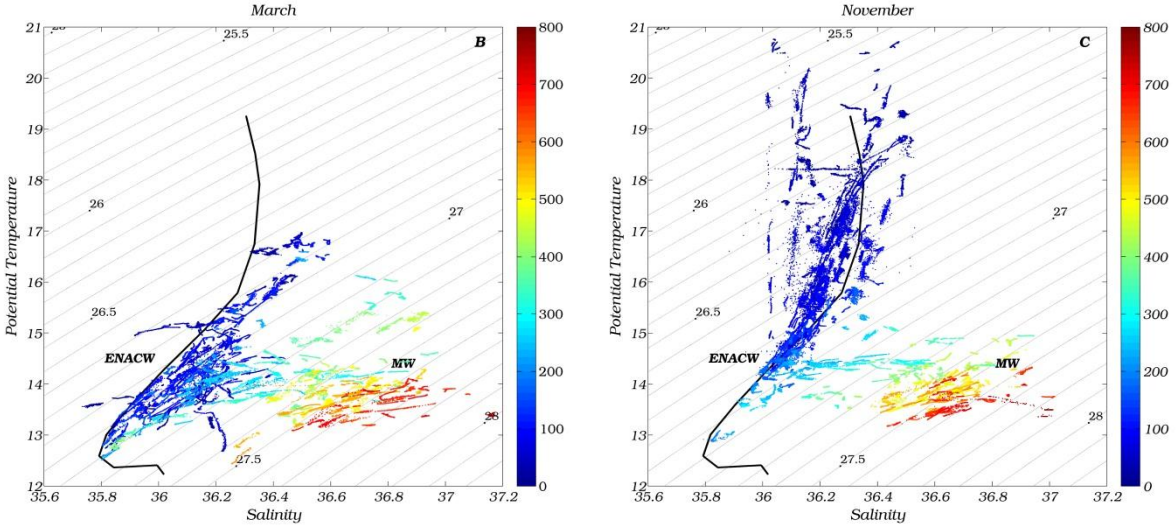

Figure 3: (cont.) (B) March. (C) November. Colorbar indicates depth (m). Black line indicates the climatological mean θ-S curve.

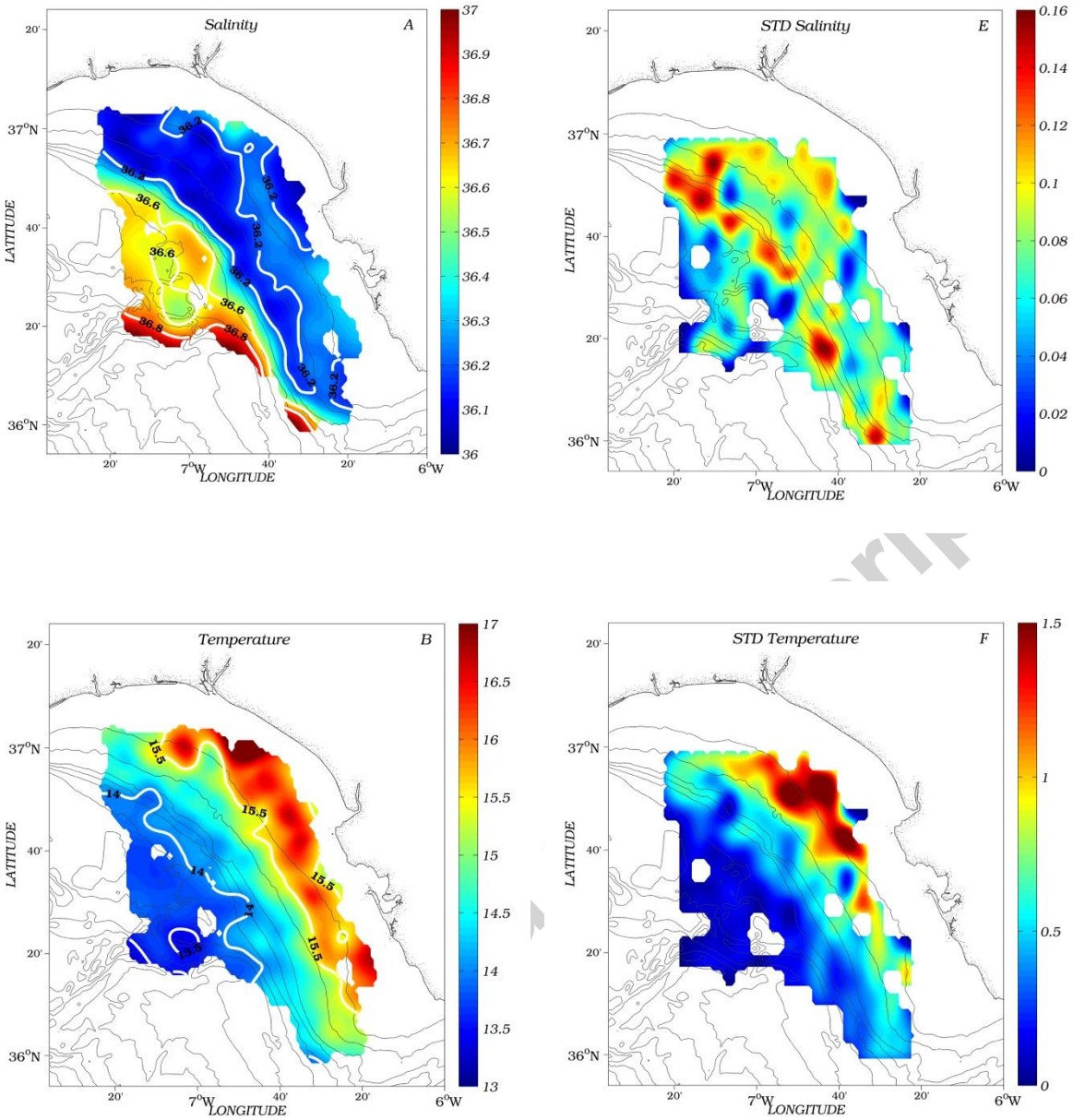
Salinity
A
STD Salinity
E
Temperature
B
STD Temperature
F
LATITUDE
LONGITUDE
37°N
36°N
20'
40'
7°W
6°W

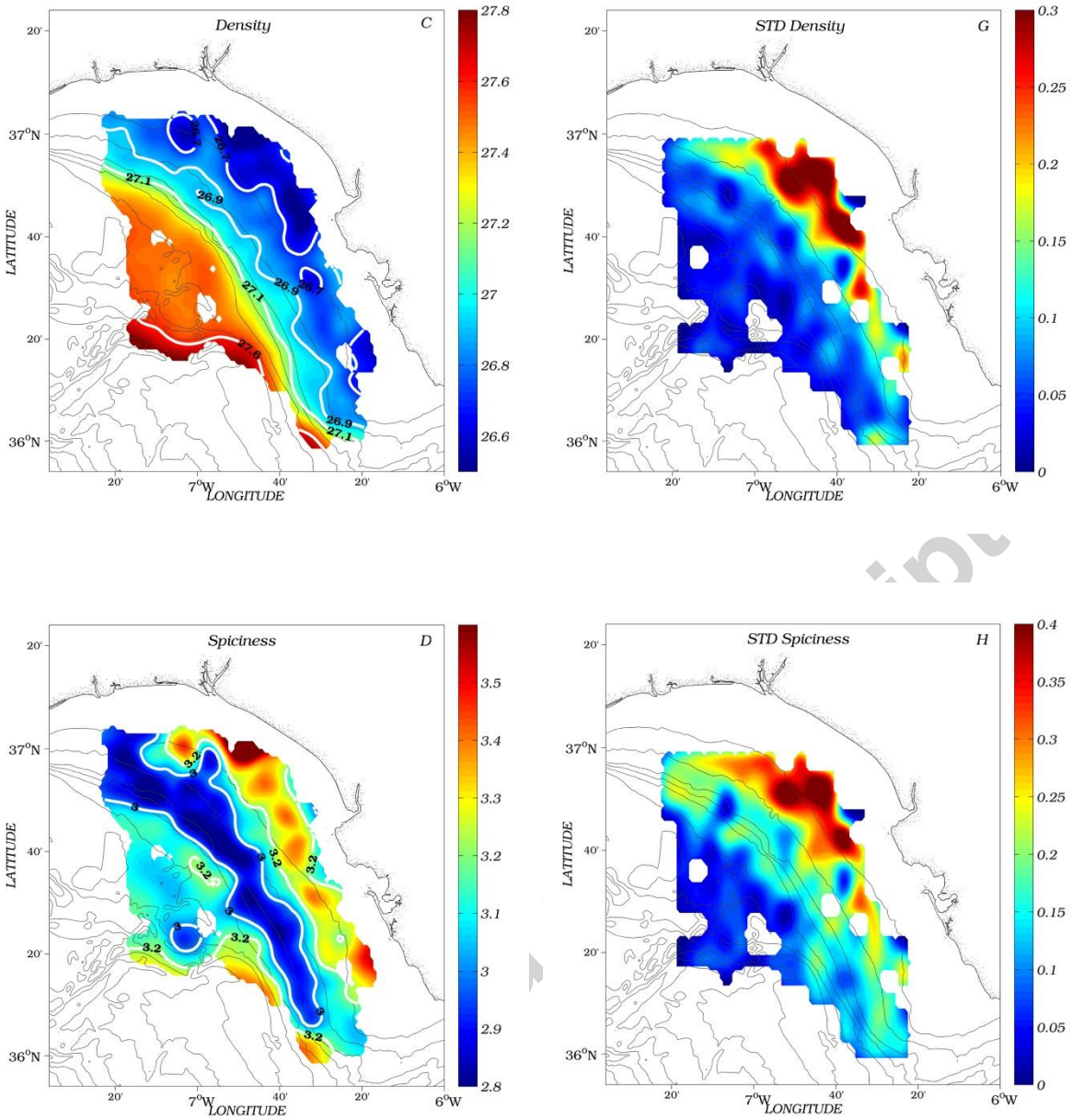

Figure 4: Mean bottom salinity (A), temperature (B), density (C) and spiciness (D) together with the respective standard deviations (E, F, G and H). Bathymetry is depicted at 100 m intervals. The 50 m isobath is also shown. Note the different colorbar ranges for each of the std fields.

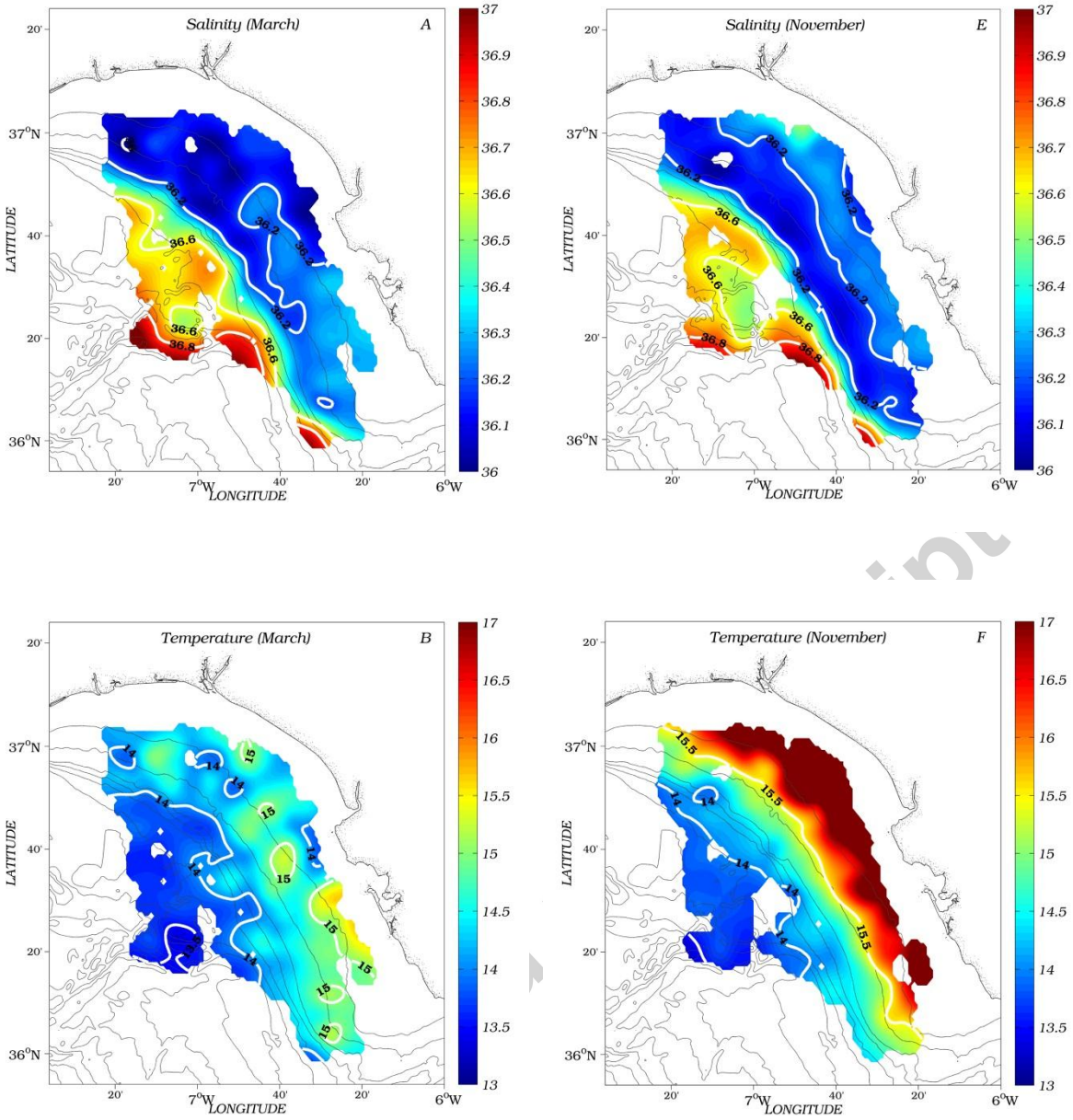

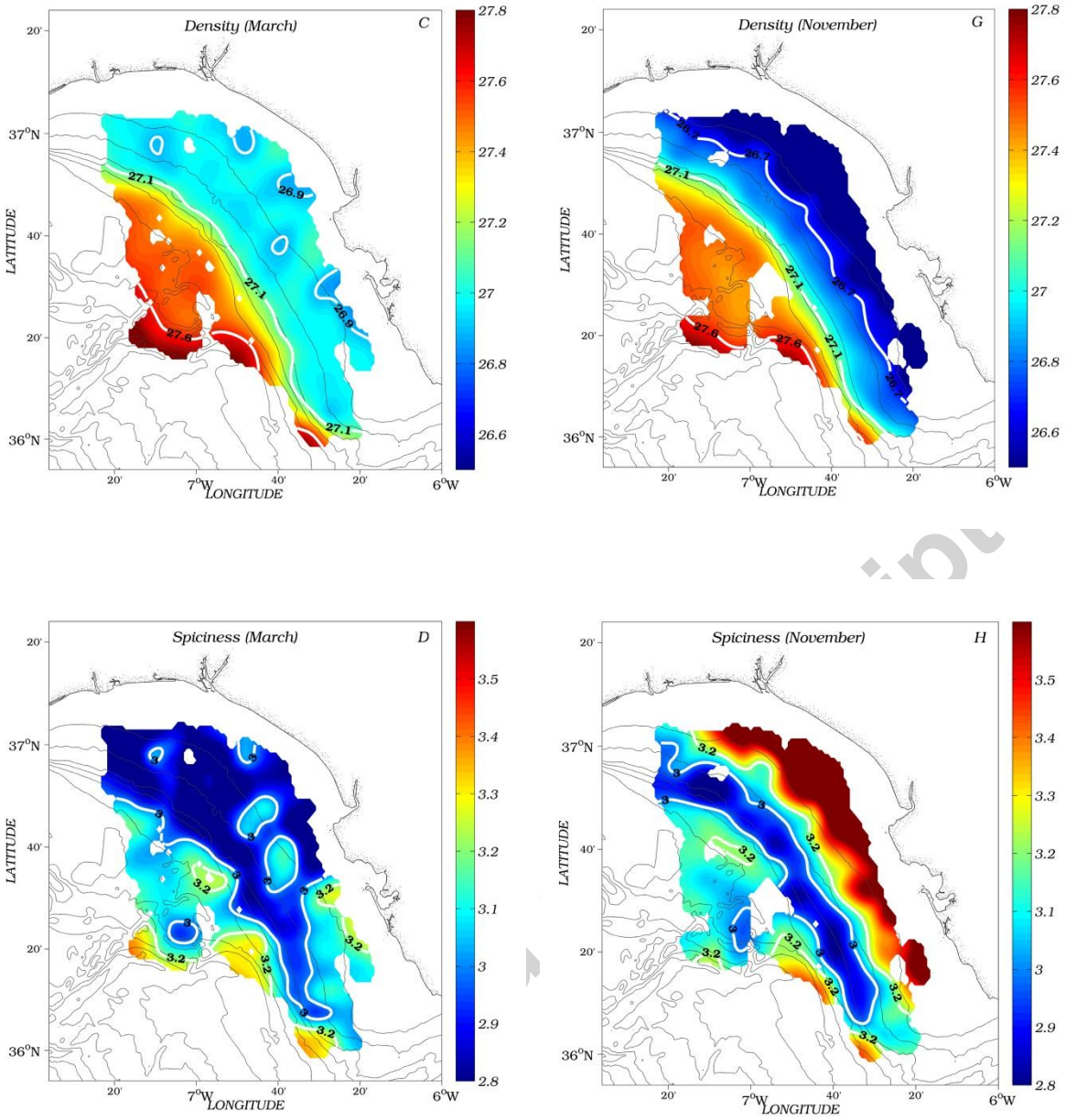

Figure 5: March salinity (A), temperature (B) density (C) and spiciness (D). November salinity (E), temperature (F), density (G) and spiciness (H). Bathymetry is depicted at 100 m intervals. The 50 m isobath is also shown.

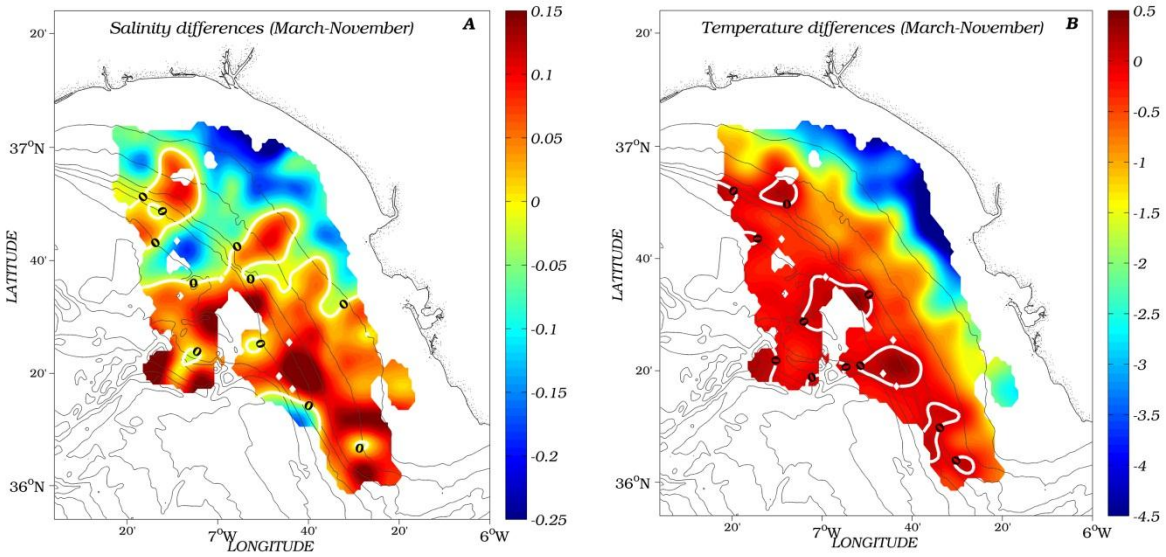

Figure 6: Mean bottom (March-November) salinity differences (A) and mean bottom (March-November) temperature differences (B). Bathymetry is depicted at 100 m intervals. The 50 m isobath is also shown.

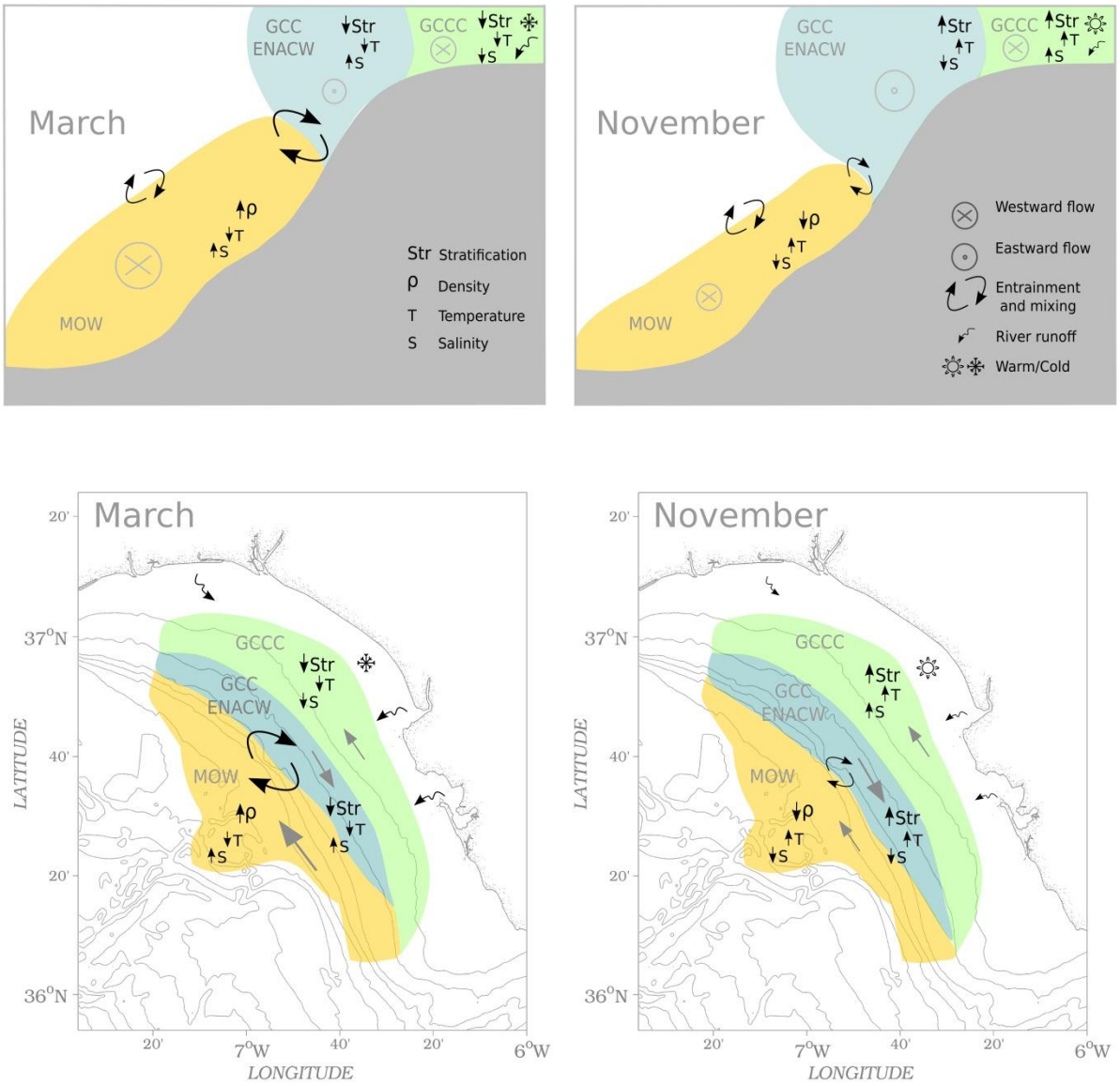

Figure 7. Vertical (top panels) and horizontal (bottom panels) sketches of March (left panels) and November near-bottom patterns deduced from the results of this paper and the literature review. GCCC represents the Gulf of Cadiz Coastal Counter Current (Relvas and Barton, 2002; Teles-Machado et al., 2009); GCC, the Gulf of Cadiz Current (Peliz et al., 2007) and MOW Mediterranean Outflow Water (Baringer and Price, 1997). Arrows indicate entrainment, detrainment (Marutitzen et al., 2001) and mixing between ENACW and MOW. In horizontal sketches, gray arrows indicate the direction and relative strength of the flow as deduced from observations presented in this paper.

Table 1: Series of cruises with date, number of hauls and number of observations per cruise.

Cruise	Date	Number of hauls	Total observations
ARSA March 2005	01-03-2005 / 11-03-2005	40	7044
ARSA November 2005	05-11-2005 / 16-11-2005	39	11582
ARSA March 2006	10-03-2006 / 20-03-2006	39	11509
ARSA November 2006	06-11-2006 / 16-11-2006	41	11907
ARSA March 2007	28-02-2007 / 09-03-2007	37	10224
ARSA November 2007	15-11-2007 / 23-11-2007	40	11790
ARSA March 2008	10-03-2008 / 20-03-2008	38	10436
ARSA November 2008	31-10-2008 / 12-11-2008	38	10135
ARSA March 2009	06-03-2009 / 15-03-2009	42	11259
ARSA November 2009	10-11-2009 / 22-11-2009	45	11845
ARSA March 2010	04-03-2010 / 11-03-2010	37	9973
ARSA November 2010	06-11-2010 / 19-11-2010	43	11357
ARSA March 2011	09-03-2011 / 18-03-2011	37	10619
ARSA November 2011	10-11-2011 / 20-11-2011	37	9553
ARSA March 2012	19-03-2012 / 26-03-2012	26	6955
ARSA November 2012	03-11-2012 / 17-11-2012	37	11085
ARSA February 2013	19-02-2013 / 28-02-2013	37	11414
ARSA November 2013	01-11-2013 / 13-11-2013	41	13320
ARSA February 2014	22-02-2014 / 03-03-2014	39	11794
ARSA November 2014	27-10-2014 / 08-11-2014	46	13983
ARSA February 2015	24-02-2015 / 03-05-2015	40	11938
	Total	819	216617

Table 2: Area-averaged mean and lower and upper bounds of the 95% confidence intervals (2.5% and 97.5% values of the normal distribution, respectively**)** calculated for the inner shelf, ENACW and MOW domains for March and November. Results of two-sample t-tests to check the statistical validity of the March-November differences both for temperature and salinity are also included.

		Salinity			**Temperature(ºC)**		
	Depth (m)	**March**	**November**	**T-Test**	**March**	**November**	**T-Test**
Inner	< 60	36.17	36.26	Sig 99%	14.65	17.78	Sig 99%
Shelf		36.13-36.20	36.24-36.29	p < 0.01	14.45-14.85	17.47-18.09	p < 0.01
ENACW	100-250	36.17	36.12	Sig 95%	14.41	14.78	Sig 95%
domain		36.13-36.20	36.10-36.14	p < 0.05	14.21-4.60	14.65-14.91	p < 0.05
MOW	> 300	36.64	36.60	Sig 90%	13.90	14.01	Sig 90%
domain		36.61-36.68	36.57-36.63	p < 0.1	13.79-14.00	13.94-14.08	p < 0.1